Paper ID ICLASS06-280

HEAT TRANSFER OF SINGLE CRYOGEN DROPLET IMPACT ONTO EPOXY SKIN PHANTOM

Jie Liu[1], Wangcun Jia[2], Henry Vu[3] and Guillermo Aguilar[4]

[1]Graduate Student, Dept of Mechanical Engineering, University of California-Riverside, liuj@engr.ucr.edu
[2]Post Doctor, Beckman Laser Institute, University of California Irvine, wjia@uci.edu
[3]Graduate Student, Dept. of Mechanical Engineering, University of California-Riverside hvu@engr.ucr.edu;
[4] Assistant Professor, Dept. of Mechanical Engineering, University of California-Riverside, gaguilar@engr.ucr.edu

ABSTRACT Cryogen Spray Cooling (CSC) is an auxiliary procedure that pre-cools the epidermis during Laser Dermatologic Surgery (LDS) to avoid non-specific epidermal thermal damage. During CSC, explosive atomization, in-flight evaporation and droplet-substrate interaction affect heat extraction from the substrate. In order to understand the heat transfer mechanism of this complex process, we study the heat transfer between a single cryogen (R134a) droplet and an epoxy skin phantom. In a high pressure chamber, cryogen droplets impact onto a skin phantom instrumented with a fast-response thin-film thermocouple. The surface temperature variations were recorded and used to calculate surface heat fluxes. Using this setup, we performed experiments to study the effects of initial surface temperature, droplet size and droplet velocity on the cooling efficiency of a cryogen droplet. Based on the experimental results, a simple model was developed to approximately estimate the heat flux between the cryogen droplet and skin phantom during impact process. The results show that the cooling efficiency increases with increasing initial substrate temperature and increasing droplet impact velocity, but the effect of the droplet size is weak.

Keywords: Cryogen Droplet, Impact, Skin Phantom, Heat Transfer

1. INTRODUCTION

Laser dermatological surgery (LDS) is the treatment of choice for vascular lesions (e.g., hemangiomas [1] and Port Wine Stain (PWS) [2] birthmarks) as well as aesthetic purpose (e.g., hair [3] and tattoo [4] removal). For these conditions, cryogen spray cooling (CSC) is an essential auxiliary method that protects the epidermis from excessive thermal damage during laser irradiation, while the target, such as PWS blood vessels located 100–500 μm below the skin surface [5] are thermally photocoagulated. The only cryogen used for this purpose thus far, approved by the FDA [3], is Tetrafluoroethane-1,1,1,2 (R134a), with a boiling temperature of -26 ^{o}C at atmospheric pressure. Short cryogen spurts (20–100 ms) [6, 7] are released from a pressurized container through a spray valve/nozzle system. Well-atomized cryogen droplets with diameters of 3–20 μm [8] and velocities 10–60 m/s [9] impact onto human skin and extract heat as they spread and evaporate.

Until now, most studies of CSC applied to human skin have assessed the cooling efficiency of a variety of nozzles and/or spraying conditions but assuming or establishing the same initial skin phantom temperature, i.e., room (20^{o}C) or normal skin temperature (~30^{o}C). Recently, however, a new technique consisting of pre-heating skin for a few seconds prior to CSC and laser irradiation was introduced [10]. The ultimate objective of this approach is to elevate sufficiently the temperature of whole skin, including the deep targeted blood vessels, so lower laser energy is required to reach the threshold for damage. For this approach to work, however, it was necessary to prove that the epidermal cooling provided by CSC nozzles could be at least as efficient as with normal initial temperature conditions. Using an aluminum foil sensor, it was shown [10] that similar minimal epidermal temperature and thus, higher surface heat fluxes could be reached regardless of the initial skin temperature. A subsequent numerical study [11] suggested that the short period of pre-heating could indeed improve the therapeutic results.

In this study, we aim at providing some insight into the cooling mechanism that dominates the heat extraction process during CSC and provide information for optimization of CSC. For this purpose, we pre-heat a skin phantom (epoxy substrate) to a steady temperature above normal skin temperature. Then we use one single cryogen droplet at T_O ~12^{o}C, which is impact onto a custom-made fast response nickel–copper thin film thermocouple (TFTC) to measure the dynamic temperature variation with droplet size (D) and velocity (V). Subsequently, we calculate the heat flux between the cryogen droplet and the skin phantom.

2. EXPERIMENTAL APPROACHES

To study the heat transfer phenomena between a single cryogen droplet and skin phantom, we conducted our experiments inside a high pressure chamber to control or reduce the evaporation of cryogen at room temperature. Figure 1 shows the schematic of the experimental facilities. Prior to the experiments, the aluminium chamber (11) with acrylic glass windows for imaging and illumination was pressurized to 6.21 bar (T_{sat} = 27 ^{o}C), which is higher than

the saturation pressure of cryogen (R-134a) at room temperature (5.71 bar). A Teflon insulator (1) that holds the heating system (2) and skin phantom with TFTC (4) on the top surface is mounted on the translation stage (12) that is used to align the nozzle (5) and TFTC. The cryogen droplets were formed at the tip of small nozzles, which were attached to a needle valve (6) connected to a small cryogen tank (7) pressurized slightly above the chamber's pressure (6.42 bar). The different impact velocity was obtained by changing the distance between the nozzle tip and the TFTC.

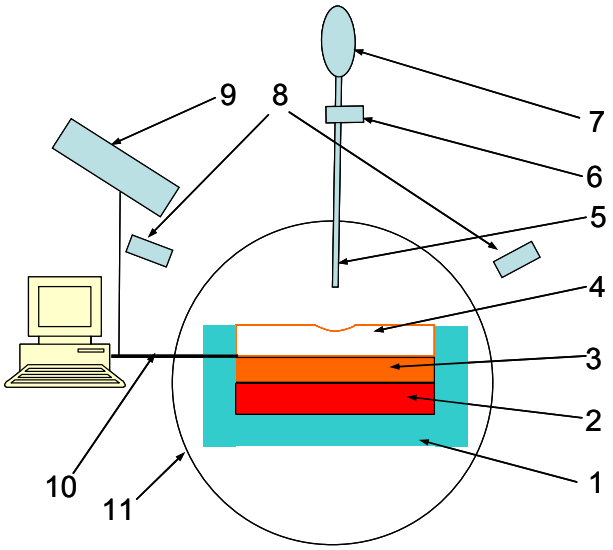

Figure 1. Experimental setup. (1) Teflon insulator, (2) Heater, (3) Heat distributor, (4) Epoxy substrate with TFTC on top surface, (5) Nozzle, (6) Needle valve, (7) Cryogen reservoir, (8). Illuminator, (9) High-speed camera, (10) Data acquisition and control cable, (11) High pressure chamber, and (12) Translation stage.

The skin phantom is made of a mixture of 3100 epoxy resin and A210 Hardener (RBC Industries, Inc., Warwick, RI) with a ratio of 3:1 in weight. The heat conductivity, capacity and density of the epoxy substrate are close to those of the human skin [11]. A spherical-cap shaped indentation (3 mm in depth and 4 mm in radius) that is used to make the cryogen stay on the joint of TFTC was made on the center of the skin phantom. The top surface and the indentation were first polished and cleaned. Thereafter the thin-film strips of copper and nickel were deposited sequentially using an E-beam evaporator system (model CV-14, Airco/Temescale). These two strips have a width of 0.5 mm and thickness of 1 μm, respectively and they are overlapped at the center of the indentation, where the droplet is deposited.

Since the TFTC is not a standard thermocouple, we calibrated it by submerging the entire substrate into a liquid bath (model RTE210, Thermo Electron Co.). The temperature of the liquid bath was measured with a K-type thermocouple (model 5TC-KK-(K)-24, OMEGA Engineering, Inc.) and the voltage output of the TFTC was recorded with a data acquisition system (iNet 100, Omega Engineering, Inc.). Figure 2 shows the variation of the voltage output with temperature. As seen, it shows a reasonably good linear relationship for the range of temperatures presented herein (-20°C to 30°C), which may be represented by:

$$T(^{o}C) = 49841 \times \mathrm{X(V)} + 34 \,. \qquad (1)$$

This TFTC is designed to measure the surface temperature and has two advantages. First, the response time is less than 50 μs [12], therefore it can measure the dynamic temperature change between cryogen and surface. Second, the metal layer is only 1 μm in thickness and with a size of 0.5 mm × 0.5 mm, thus it creates a minimal disturbance to heat flow across the surface.

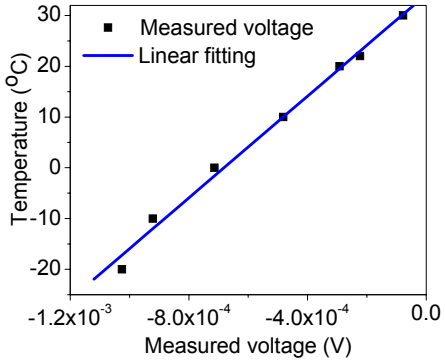

Figure 2. Measured voltages (V) vs. corresponding temperature (°C).

Once the surface temperature history is obtained with the TFTC, the heat flux at the surface can then be conveniently obtained using the one-dimensional, semi-infinite medium solution for a step change in surface temperature and applying Duhamel's superposition integral [13, 14].

3. RESULTS

3.1 Effects of the T_O

Figure 3 shows the measured temperature variation with time for different T_O with D = 2.4 mm and V = 2.4 mm. For the four different initial temperatures shown herein, it is seen that the surface temperature drops quickly once the cryogen droplet establishes contact with the skin phantom. The maximum measured temperature drop ΔT is 12, 14, 15 and 16 °C for T_O at 31, 35, 39 and 45 °C respectively. After the temperature sharp decrease periods, a considerable stable temperature can be observed because of the slow evaporation of the cryogen droplet. This period is called as life time (τ) of the cryogen droplet, which is defined as the time from the lowest temperature to the point where the temperature begins to increase steadily. τ is about 2.6, 1.3, 1.2 and 1.1 second for T_O at 31, 35, 39 and 45 °C respectively.

Figure 4 shows the heat flux variation with time for different T_O with D = 2.4 mm and V = 2.4 mm according to the temperature variation shown in Figure 3 during the drastic temperature droplet period. A noticeable increase in the maximum heat flux is appreciated as the initial temperature increases. For the lowest and highest initial temperatures (31 and 45 °C, respectively) the maximum heat fluxes q_{max}'' are 118 and 220 kW/m^2, respectively.

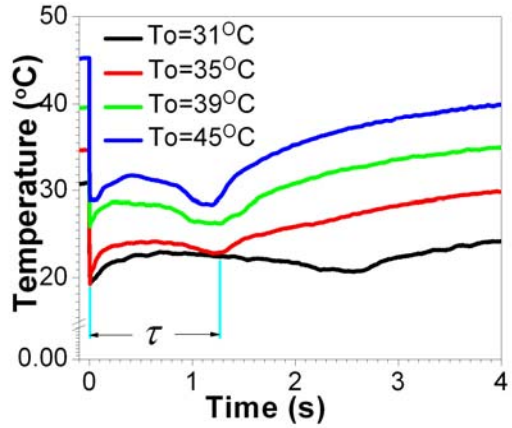

Figure 3. Temperature variation with different T_O with D = 2.4 mm and V = 2.4 m/s.

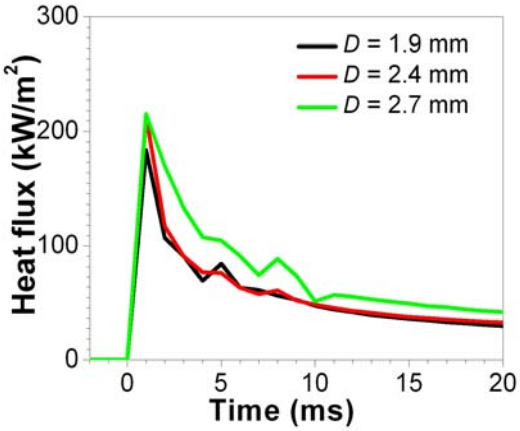

Figure 6. Heat flux variation with difference droplet size with T_O = 45 ^{O}C and V = 2.4 m/s

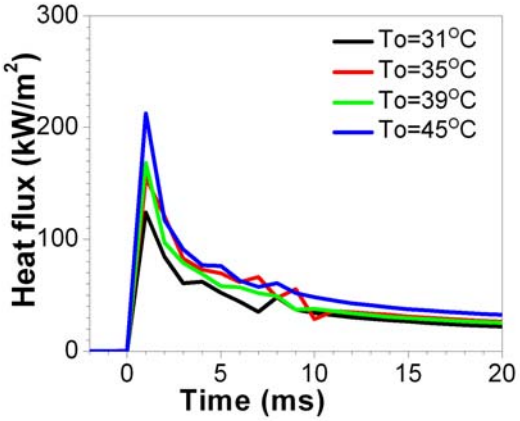

Figure 4. Heat flux variation with difference T_O with D = 2.4 mm and V = 2.4 m/s.

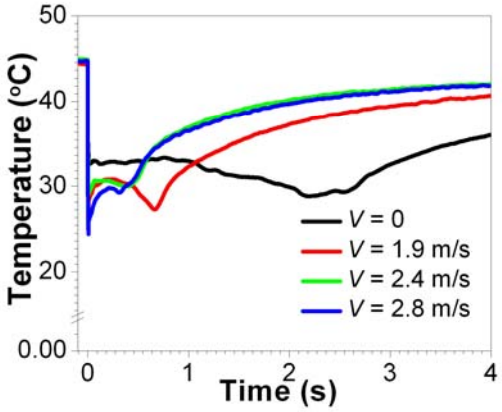

Figure 7. Temperature variation with difference V with T_O = 45 ^{O}C and D = 1.9 mm.

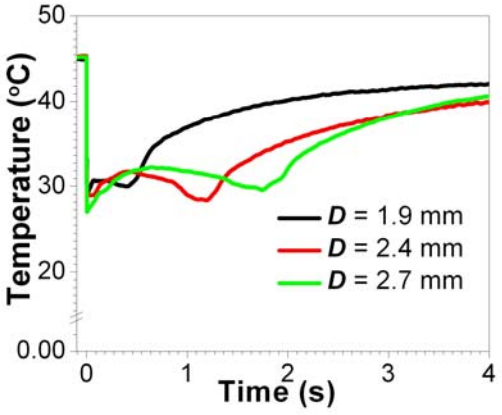

Figure 5. Temperature variation with difference droplet size with T_O = 45 ^{O}C and V = 2.4 m/s.

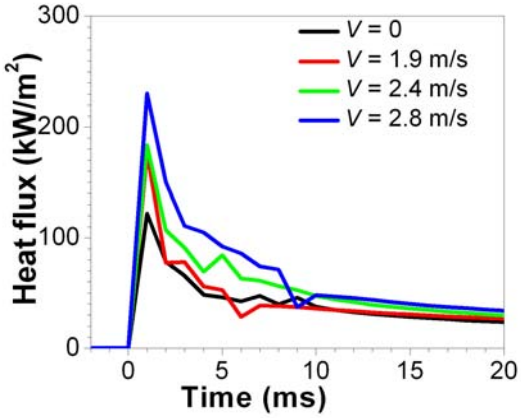

Figure 8. Heat flux variation with difference V with T_O = 45 ^{O}C and D = 1.9 mm.

3.2 Effects of the Droplet Size *D*

Figure 5 shows the measured temperature variation with time for different droplet size D with initial temperature at 45 ^{O}C and V = 2.4 m/s. ΔT is almost the same for all three D, but the τ is 1.8, 1.3 and 0.6 s for D = 2.7, 2.4 and 1.9 respectively.

Figure 6 shows the corresponding variation of the heat flux for three different sizes according to Figure 5. It shows that the maximum heat fluxes q_{max}" are similar for all three droplet sizes.

3.3 Effects of the Droplet Velocity *V*

Figure 7 shows the measured temperature variation with different V with T_O = 45 ^{O}C and D = 2.4 mm. It shows that the V affects not only ΔT but also the life time. The ΔT is 12 and 19 ^{o}C for V = 0 and 2.8 m/s respectively. τ is 2.6 and 0.4 s for V = 0 and 2.8 m/s respectively. Figure 8 shows the corresponding variation of the heat flux for V with range from 0 to 2.8 m/s. The effect of V on q_{max}" is preeminent. The heat flux is 120 and 240 kW/m2 for V = 0 and 2.8 m/s, respectively.

4. DISSUSION

Figures 3 and 4 show that as T_O increases, ΔT and q_{max}" increases too. These observations are consistent and qualitatively similar to those previously reported by Jia *et al.*[10]. Figure 9 shows the heat transfer coefficient (h) is same at 6.8 kW/(m^2 K) for different T_O with D = 2.4 mm and V = 2.4 m/s. It demonstrates that heat transfer is independent of T_O. Thus, the heat flux is highest for T_O because it has largest ΔT. Also in Figure 4, it is shown that increasing T_O the life time τ decreases because the evaporation rate increases with higher temperature.

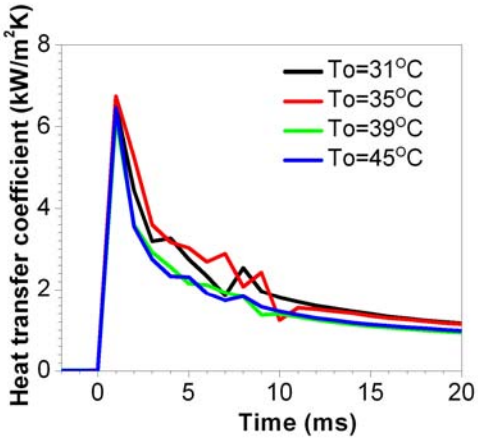

Figure 9. Heat transfer coefficient for different T_O with D = 2.4 mm and V = 2.4 m/s

Figures 5 and 6 show that the droplet size does not affect the ΔT and the q_{max}". This phenomenon, also illustrated in Figure 10 shows that h is independent of droplet size D. Furthermore, both V and T_O are constant in this case, whiel the maximum heat flux is the same for different D. The larger D the more mass of cryogen droplet, therefore, for the same surface temperature, the cryogen needs more time to evaporate. In other words, τ increases as the D increases.

Figures 7 and 8 show that both ΔT and q_{max}" increase as the V increases with same T_O and D. Figure 10 shows the heat transfer coefficient increases as V increases. For V = 0, only conduction heat transfer occurs and the heat transfer coefficient is only 3.8 kW/(m^{2}K). As V increases, the effects of convection heat transfer becomes more prominent, and when V = 2.8 m/s, the heat transfer value can reach 7.2 kW/(m^2 K). This means that the convection heat transfer is more efficient to extract heat from the skin phantom than conduction heat transfer during the cryogen impact process. Thus, the evaporation time will be shortened and results in shorter τ as V increases.

From the above experimental results, we can say that the heat transfer between the cryogen droplet and indented skin phantom is related to T_O, D and V. Therefore, a simple model is developed to predict the average heat flux (q") during the impact process based on previous research of heat transfer on the impact of droplet onto a flat surface using the thermal boundary layer theorem.

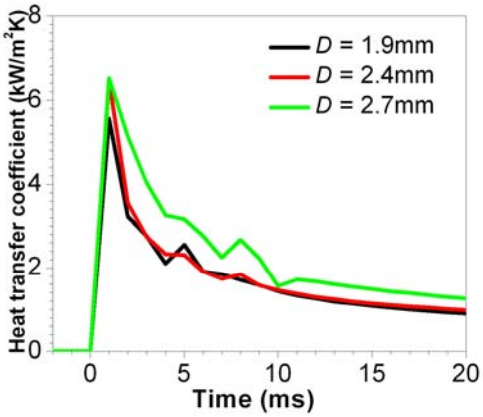

Figure 10. Heat transfer coefficient for different D with T_O = 45 ^{O}C and V = 2.4 m/s

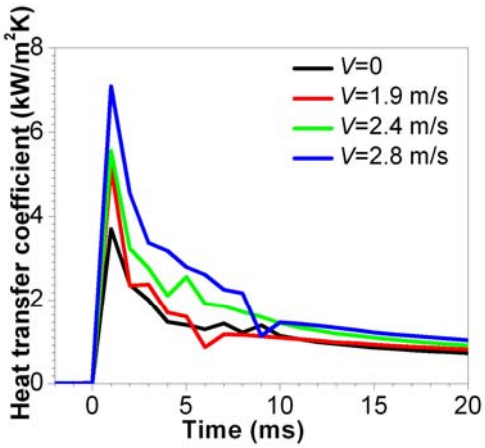

Figure 11. Heat transfer coefficient for different V with T_O = 45 ^{O}C and D = 1.9 mm.

Considering the droplet impact onto flat surface as axisymmetric flow, Pasadideh-Fard M. *et al* [15] proposed the thickness of boundary layer δ_u of the cryogen droplet:

$$\delta_u = \frac{2D}{\sqrt{Re}} \quad (2)$$

The thermal boundary δ_u is [16]:

$$\delta_T = \frac{\delta_u}{Pr^{0.4}} \quad (3)$$

Inserting Eq. (2) into Eq. (3)

$$\delta_T = \frac{2D}{Pr^{0.4}\, Re^{0.5}} \quad (4)$$

Where $Re = \frac{\rho V D}{\mu}$ and $Pr = \frac{\nu}{\alpha}$.

Thus, the *q"* during the impact process can be expressed as:

$$q'' = k\frac{\Delta T}{\delta_T} = \frac{\Delta T}{2D} Nu\,, \quad (5)$$

Where

$$Nu = Pr^{0.4}\, Re^{0.5}\,. \quad (6)$$

The model above is only suitable for droplets with certain velocity impact onto flat surface. It is not suitable for $V = 0$ and indented surface in this study, thus a modified format of *Nu* is proposed:

$$Nu = C_1 + C_2 (Pr^{0.4}\, Re^{0.5})^{C_3}\,, \quad (7)$$

where C_1 accounts for the conduction heat transfer with $V = 0$, and C_2 and C_3 are added to modify the discrepancy between flat and indented surface. To find the coefficients in Eq. (7), the experimental results in Table 1. were used. The heat flux *q"* in this study accounts for the average heat flux over the first 6 ms from the beginning of temperature drop [17]. The highlighted rows were used to find the coefficients using Eq. (5) and (7) and data in other rows were used to test the proposed model. The final format of *Nu* is:

$$Nu = 98 + 0.15(Pr^{0.4}\, Re^{0.5})^{1.06} \quad (8)$$

Figure 12 shows the comparison of experimental results with model predicted results. It shows that the majority of experimental results and model predicted results fit well. The maximum error between the experimental results and model predication are below 30%. The errors are caused by the inaccuracy of the experimental results and using the smooth method especially for high heat flux zone.

Figure 13 shows the comparison of the effects of ΔT between experimental results and model prediction with D = 2.4 mm and different V. It demonstrates that the *q"* increases linearly with ΔT because *Nu* is constant with fixed D and V in Eq. (8). Therefore, the *q"* in Eq. (6) linearly increases with ΔT, but the *q"* increased due to the increased ΔT is different for four V values. For $V = 0$, the *q"* changes with ΔT varying from 0 to 40 ^{O}C is about 70 kW/m^2, but for V= 2.7 m/s, the *q"* can reach 150 kW/m^2.

Table 1. The experimental parameters and results of *q"*

	V = 0 m/s		V =1.9 m/s		V = 2.4 m/s		V = 2.8 m/s	
	T_O (^{o}C)	*q"* (kW/m^2)	T_O (^{o}C)	*q"* (kW/m^2)	T_O (^{o}C)	*q"* (kW/m^2)	T_O (^{o}C)	*q"* (kW/m^2)
1.9 mm	31	46	31	67	31	76	31	63
	35	61	35	73	35	83	35	73
	39	62	39	92	39	88	39	84
	45	67	45	112	45	99	45	115
2.4 mm	31	44	31	54	31	71	31	76
	35	58	35	75	35	83	35	96
	39	64	39	87	39	88	39	111
	45	71	45	98	45	106	45	125
2.7 mm	31	54	31	70	31	64	Break up	
	35	63	35	91	35	83	Break up	
	39	72	39	93	39	100	Break up	
	45	83	45	113	45	127	Break up	

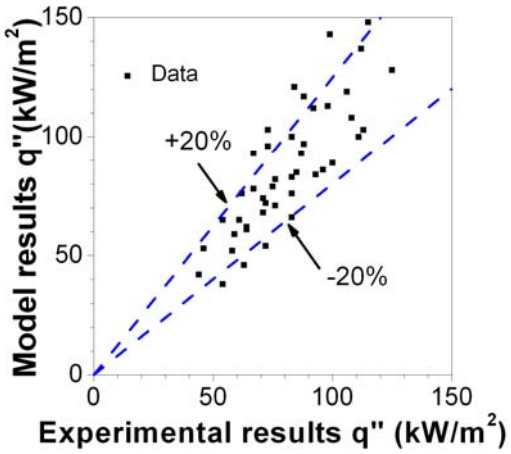

Figure 12. Comparison of experimental results with model predicted heat flux *q"*.

Figure 13 shows the comparison of the effects of ΔT between experimental results and model prediction with D = 2.4 mm and different V. It demonstrates that the *q"* increases linearly with ΔT because *Nu* is constant with fixed D and V in Eq. (8). Therefore, the *q"* in Eq. (6) linearly increases with ΔT, but the *q"* increased due to the increased ΔT is different for four V values. For $V = 0$, the *q"* changes with ΔT varying from 0 to 40 ^{O}C is about 70 kW/m^2, but for V= 2.7 m/s, the *q"* can reach 150 kW/m^2.

Figure 14 shows the comparison of effects of V between experimental results and model results where D = 2.4 mm and different T_O. Apparently, the *q"* increases in the order of $Re^{0..5}$ with fixed D and T_O. It also shows that as the T_O

increases, the effect of V becomes prominent. For instance, with T_O = 31 ^{O}C, the percentage of increased q'' due to the V increases from 0 to 3m/s is, which is less than 20%. When T_O = 45 ^{O}C, this percentage is almost 50%.

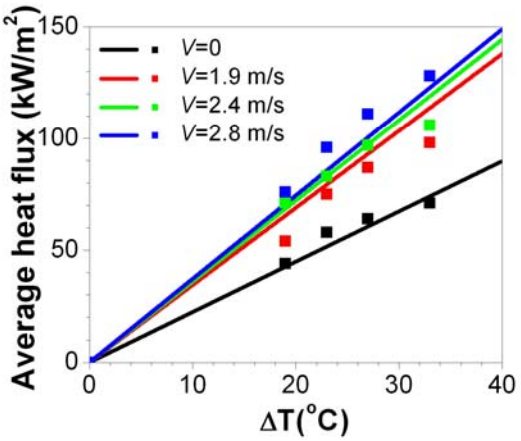

Figure 13. Experimental results and model predicted effect of ΔT with D = 2.4 mm and different V.

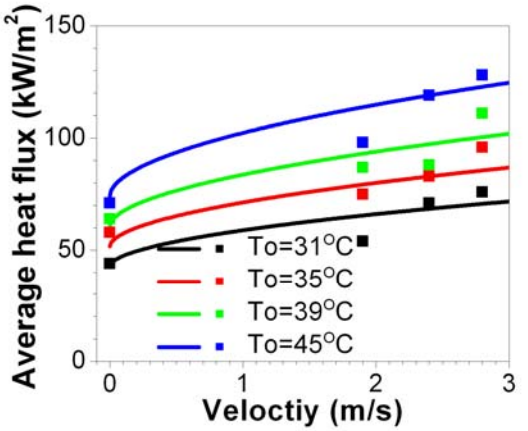

Figure 14. Experimental results and model predicted effect of V with D = 2.4 mm and different ΔT.

5. CONCLUSION

Both experimental results and model predictions show that as the initial surface temperature T_O and droplet velocity V increases, the heat transfer between the cryogen droplet and skin phantom enhances. The droplet size, D, has a weak effect on the heat transfer between cryogen droplets and skin phantoms during the impact process.

NOMENCLATURE

D	droplet diameter [mm]
h	Heat transfer coefficient [kW/(m^2 K)]
Nu	Nussle number
Pr	Prandtl number (ν/α)
q''	average heat flux during impact [kW/m^2]
q''_{max}	maximum heat flux during impact [kW/m^2]
Re	Reynolds number ($\rho VD/\eta$)
T_O	initial temperature [^{o}C]
V	droplet velocity [m/s]

Greek symbol

α	thermal diffusivity [m^2/s]
δ_T	thermal boundary layer thickness [mm]
δ_u	velocity boundary layer thickness [mm]
ΔT	temperature drop [^{o}C]
ν	kinetic viscosity [m^2/s]
ρ	density [kg/m^3]
τ	life time of cryogen droplet [s]

REFERENCES

1. Kelly, K.M., Nelson, J.S., Lask, G.P., Geronemus, R.G., and Bernstein, L.J.,"Cryogen Spray Cooling in Combination with Nonablative Laser Treatment of Facial Rhytides," Archives of Dermatology, Vol. 135(6), pp. 691-694. 1999
2. Nelson, J.S., Milner, T.E., Anvari, B., Tanenbaum, B.S., Kimel, S., Svaasand, L.O., and Jacques, S.L.,"Dynamic Epidermal Cooling During Pulse-Laser Treatment of Port-Wine Stain-a New Methodology with Preliminary Clinical Evaluation," Achives of Dermatology, Vol. 131(6), pp. 695-700. 1995
3. Goldman, M.P. and Fitzpatrick, R.E., 1999, Cutaneous Laser Surgery, Mosby, Chicago.
4. Nelson, J.S., Milner, T.E., Anvari, B., Tanenbaum, B.S., Kimel, S., Svaasand, L.O., and Jacques, S.L.,"Selective Photothermolysis and Removal of Cutaneous Vasculopthies and Tattoos by Pulsed Laser," Plastic and Reconstructive Surgery, Vol. 88(4), pp. 723-731. 1991
5. Anvari, B., Milner, T.E., Tanenbaum, B.S., Kimel, S., Svaasand, L.O., and Nelson, J.S.,"Dynamic Epidermal Cooling in Conjunction with Laser Treatment of Port-Wine Stains: Theoretical and Preliminary Clinical Evaluations," Laser in Medical Science, Vol. 10(5), pp. 105-112. 1995
6. Aguilar, G., Majaron, B., Pope, K., Svaasand, L.O., Lavernia, E.J., and Nelson, J.S.,"Influence of Nozzle-to-Skin Distance in Cryogen Spray Cooling for Dermatologic Laser Surgery," Lasers in Surgery and Medicine, Vol. 28(2), pp. 113-120. 2001
7. Aguilar, G., Vu, H., and Nelson, J.S.,"Influence of Angle between the Nozzle and Skin Surface on the Heat Flux and Overall Heat Extraction During Cryogen Spray Cooling," Physics in Medicine and Biology, Vol. 49(10), pp. N147-N153. 2004
8. Aguilar, G., Majaron, B., Verkruysse, W., Zhou, Y., Nelson, J.S., and Lavernia, E.J.,"Theoretical and Experimental Analysis of Droplet Diameter, Temperature, and Evaporation Rate Evolution in Cryogenic Sprays," International Journal of Heat and Mass Transfer, Vol. 44(17), pp. 3201-3211. 2001
9. Aguilar, G., Majaron, B., Karapetian, E., Lavernia, E.J., and Nelson, J.S.,"Experimental Study of Cryogen Spray Properties for Application in Dermatologic Laser Surgery," IEEE Transactions on Biomedical Engineering, Vol. 50(7), pp. 863-869. 2003
10. Jia, W.C., Aguilar, G., Wang, G.X., and Nelson, J.S.,"Heat-Transfer Dynamics During Cryogen Spray Cooling of Substrate at Different Initial Temperatures,"

Physics in Medicine and Biology, Vol. 49(23), pp. 5295-5308. 2004
11. Jia, W.C., Aguilar, G., Verkruysse, W., Franco, W., and Nelson, J.S.,"Improvement of Port Wine Stain Laser Therapy by Skin Preheating Prior to Cryogen Spray Cooling: A Numerical Simulation," Lasers in Surgery and Medicine, Vol. 38(2), pp. 155-162. 2006
12. Schreck, E., Fontana, R.E., and Singh, G.P.,"Thin-Film Thermocouple Sensors for Measurement of Contact Temperatures During Slider Asperity Interaction on Magnetic Recording Disks," IEEE Transactions on Magnetics, Vol. 28(5), pp. 2548-2550. 1992
13. Taler, J.,"Theory of Transient Experimental Techniques for Surface Heat Transfer," International Journal of Heat and Mass Transfer, Vol. 39(17), pp. 3733-3748. 1996
14. Franco, W., Liu, J., Wang, G.X., Nelson, J.S., and Aguilar, G.,"Radial and Temporal Variations in Surface Heat Transfer During Cryogen Spray Cooling," Physics in Medicine and Biology, Vol. 50(2), pp. 387-397. 2005
15. Pasandideh-Fard, M., Aziz, SD., Chandra, S. and Mostaghimi,"Cooling Effectiveness of a Water Droplet Impinging on a Hot Surface," International Journal of Heat and Fluid Flow, Vol. 22, pp. 201-210. 2001
16. White, F.M., 1991, Viscous Fluid Flow, McGrawHill, New York,2nd ed.
17. Liu, J., Franco, W., and Aguilar, G., "The Effect of Roughness on the Impact Dynamics and Heat Transfer of Cryogen Droplets Impinging onto Indented Skin Phantoms", 2005, in ASME-NHTC, San Francisco, CA.